Macromolecules

NOTE

pubs.acs.org/Macromolecules

Controlled Aggregation in Conjugated Polymer Nanoparticles via Organic Acid Treatments

Yoon-Joo Ko, Eladio Mendez, and Joong Ho Moon*

Department of Chemistry and Biochemistry, Florida International University, 11200 SW 8th St., Miami, Florida 33199, United States

Supporting Information

Conjugated polymers (CPs) are fluorescent materials that are useful for fluorescent microscopic imaging of cells and tissues.[1−7] Their photophysical properties, such as high molar absorptivity (ε), high quantum yield (QY), and high photostability, are suitable for the fluorescent labeling and detection of nucleic acids,[8,9] proteins,[10] enzymes,[11,12] cancer cells,[13] and bacteria.[14,15] In addition to the photophysical properties, versatile organic synthesis allows straightforward modification for absorption and emission tuning and coupling of sensing entities into CPs.[16,17] Despite these promising fundamental photophysical characteristics and successful sensing applications in vitro, cellular imaging applications of CPs have been retarded by the intrinsic hydrophobic nature of conjugated backbones, poor cellular uptake efficiency, and toxicity. Phase separation and aggregation between polymer chains in aqueous media are the most obvious limitations.[18−23] Severe aggregation generates $\pi-\pi$ stacking of conjugated backbones that significantly diminishes the physical and photophysical merits, so that the fluorescence imaging applications are no longer advantageous. To achieve aqueous solubility of CPs and decrease aggregations, various polar or charged pendant groups have been introduced into the side chains of CPs. CPs with negative charges and/or branched ethylene glycol side chains exhibit relatively high QYs, but their poor cellular uptake efficiency retards applications in imaging.[24] Positively charged CPs are taken up by live cells through ionic interaction between the CPs and the negatively charged cellular membrane followed by endocytosis pathways.[25] However, the permanent positive charges, mainly from quaternary ammonium salts, often cause cellular toxicity, limiting the cellular applications of CPs.[15] Most recently, researchers demonstrated that conjugated polymer nanoparticles (CPNs) fabricated by phase inversion precipitation,[3] encapsulation in lipids,[7] or direct emulsion polymerization[5] of nonaqueous soluble CPs are photophysically excellent and suitable for live cell imaging.

Previously, we fabricated CPNs by treating a nonaqueous soluble, primary amine-containing poly(phenylene ethynylene) (PPE-NH_2) with organic acids to overcome the above issues in cellular imaging.[2,4] We have demonstrated that organic acid treatment of PPE-NH_2 followed by ultrafiltration produces stabilized CPNs (<100 nm in hydrodynamic radius) in water, exhibiting high QYs, photostability, and uptake by live cells without noticeable toxic effects. The key discovery is that the controlled chain−chain interaction by organic acids allows formation of stable nanoparticles via balanced hydrophilicity (i.e., surface charges in the side chains) and hydrophobicity (conjugated backbones), while the photophysical properties of CPs are relatively preserved in aqueous phases. Here, we present spectroscopic evidence that different organic acid treatment results in different aggregation structures and photophysical properties of CPs in water. CPNs formed by acetic acid (AA) treatment (CPN-AAs) exhibit characteristics of loose aggregation with minimal $\pi-\pi$ stacking, while CPNs formed by tartaric acid (TA) treatment (CPN-TAs) exhibit a high degree of $\pi-\pi$ stacking among PPE-NH_2 chains. Aggregation structures (Figure 1) were suggested from various spectroscopic techniques including nuclear magnetic resonance (NMR) spectroscopic studies. Because of the dense aggregation, higher fluorescence quenching efficiency was observed in the CPN-TAs compared to that of CPN-AAs. Understanding and controlling aggregation structures will lead to broader cellular applications of CPs such as labeling of target cells with improved photophysical properties or delivery of biologically active molecules to target cells or tissues, depending on the aggregation natures.

The basic mechanism of particle formation with nonaqueous soluble CPs is phase inversion precipitation.[26] When a dilute CP solution in a water miscible solvent is added to an excess volume of water or aqueous buffer, the CPs aggregate and form particles as the organic solvent diffuses into the water phase. The particle size and stability are highly dependent on the amount of organic solvent, polymer concentration, and salinity. Indeed, when an aliquot of the PPE-NH_2 synthesized in an organic solvent [i.e., *N*-methyl-2-pyrrolidone (NMP)] was mixed with an excess amount of water without acid treatment, precipitates formed immediately from the concentrated polymer solution and after overnight stirring from the highly diluted solution. However, when the same batch of polymer at the same high concentration was pretreated with acetic or tartaric acid followed by mixing with an excess amount of water, a clear homogeneous solution was obtained. No indication of precipitation was observed in the solution even after extended stirring, dialyzing against water, and concentrating in water (more than 10 mg/mL). However, physical precipitation was observed during the dialysis when the same batch of polymer was treated with citric acid. Hydrodynamic radii measured by dynamic light scattering (DLS) indicated that the sizes of the CPNs were different (1) when the same batch of PPE-NH_2 was treated with different organic acids and (2) when different batches of polymer were treated with the same organic acids. If the mechanism of particle

Received: March 23, 2011
Revised: May 27, 2011
Published: June 08, 2011

ACS Publications © 2011 American Chemical Society

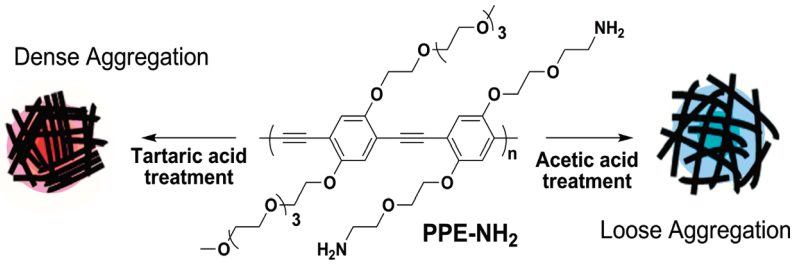

Figure 1. Schematic illustration of CPN formation. The same batch of PPE-NH_2 produces different aggregation structures depending on the organic acid treatment.

formation is the phase inversion precipitation, which is driven kinetically by the insolubility of PPE-NH_2, the hydrodynamic radii of CPNs would not be affected by counteranions and molecular weight differences between the batches. On the basis of this observation, we postulate that the formation of CPNs was not driven by the phase inversion precipitation but was driven by a different mechanism such as micelle formation, once the amine groups of the PPE were protonated by organic acids. Because the resulting PPEs-NH_3^+ typically from low molecular weight proportions increased hydrophilicity due to the acid treatment, the aggregation mechanism will follow the micelle-formation mechanism that is closely correlated with the hydrophilicity (length) of side chains, nature of counteranions, molecular weights, and salt concentration.[27] NMR studies support the concentration, temperature, and counteranion dependent aggregation behaviors of CPNs (see the NMR section below). Tartaric acid, which is a dicarboxylic acid, induces strong interchain interaction by attracting more PPE chains (both high molecular weight proportions with nonaqueous solubility and low molecular weight proportions with a limited aqueous solubility), bringing adjacent rigid-rod PPEs together to form a various sized compact particles. The particles are then stabilized by the surface positive charges, preventing further precipitation. Meanwhile, acetic acid acts as a solvent for the low molecular weight charged PPE-NH_3^+. When poor solvent water is mixed with the PPE-NH_2/acetic acid, the relatively solvated low molecular weight fractions are loosely aggregated with the rest of the polymers. Contributions from those low molecular weight proportions are observed from various spectroscopic data (see below). Because the high molecular weight proportion in both CPNs exhibits no (or very limited) aqueous solubility even after acid treatment, the aggregation of the high molecular weight proportion is neither acid nor concentration dependent. The contributions from the high molecular weight proportions were seen in both emission and NMR spectra of both CPNs. Aggregation size changes upon exchange of counterions in quaternized amine-containing poly(fluorene)s were reported previously.[28] In addition, aggregation changes in polyelectrolytes upon interaction with charged dyes or DNA were also previously observed.[29−31]

Spectroscopic analyses of the CPNs strongly indicate that the aggregation structures are significantly different for the two acid treatments (Figure 2). The CPN-AAs exhibit blue-shifted absorption and emission with a relatively narrow spectral width comparable to those of PPEs in an organic solvent.[32] Meanwhile, CPN-TAs exhibit characteristic aggregation features (red shift and broadening) in both absorption and emission spectra. Increased wavelength in the absorption results from better planarization of the conjugated backbone and/or extended conjugation through space.[33] The CPN-AAs exhibit a relatively

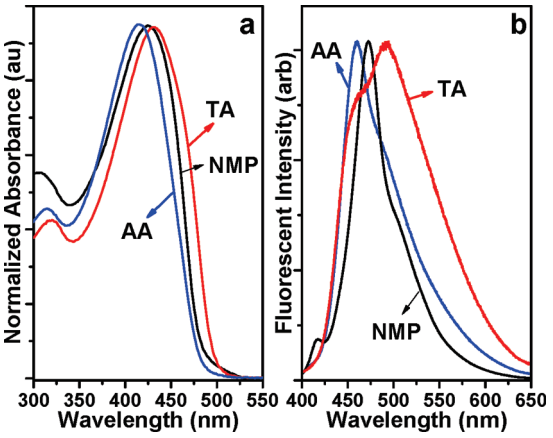

Figure 2. Absorbance (a) and emission spectra (b) of the PPE-NH_2 in NMP, CPN-AA, and CPN-TA. The same batch of PPE treated with two different acids results in different photophysical properties.

sharp absorption and slightly broadened emission spectrum compared to that of PPE-NH_2 in NMP (Figure 2), indicating a limited degree of aggregation. The spectral shape implies the presence of different aggregation stages with different excited states. Although precise assignment of each spectral feature is uncertain and requires further controlled studies by single-molecular spectroscopy,[34] the two emission spectra clearly indicate different populations of conformations or aggregation stages. Nonetheless, the CPNs exhibit high quantum yields (QYs) (0.13 for the CPN-AAs and 0.06 for the CPN-TAs) in water. As expected, CPN-TAs exhibit lower QYs than CPN-AAs due to the high degree of $\pi-\pi$ staking. Similar sharp absorption with broad emission characteristics were previously reported in the rigid hydrophilic-structured CPs in water.[35]

Different aggregations induced by the organic acids treatments were further supported by NMR spectroscopic studies. Since the protons in the CPNs are exposed to various chemical environments (i.e., different solvation and stacking among the conjugated backbones), monitoring these protons using NMR spectroscopy as a function of concentration and organic solvent will provide structural information. Typically, chemical shift and broadness of the aromatic protons that are sensitive to the $\pi-\pi$ stacking of conjugated backbones will provide information on the degree of aggregation.[36−38] Using the ultrafiltration technique equipped with a molecular weight cutoff membrane (10 kDa), we successfully exchanged the solvent (water) of CPNs with deuterium oxide without changing the aggregation status of the polymer. While broad and poorly resolved ^1H NMR spectra of the CPNs indicate that the PPE-NH_2 were aggregated in water,

dx.doi.org/10.1021/ma200661h |*Macromolecules* 2011, 44, 5527–5530

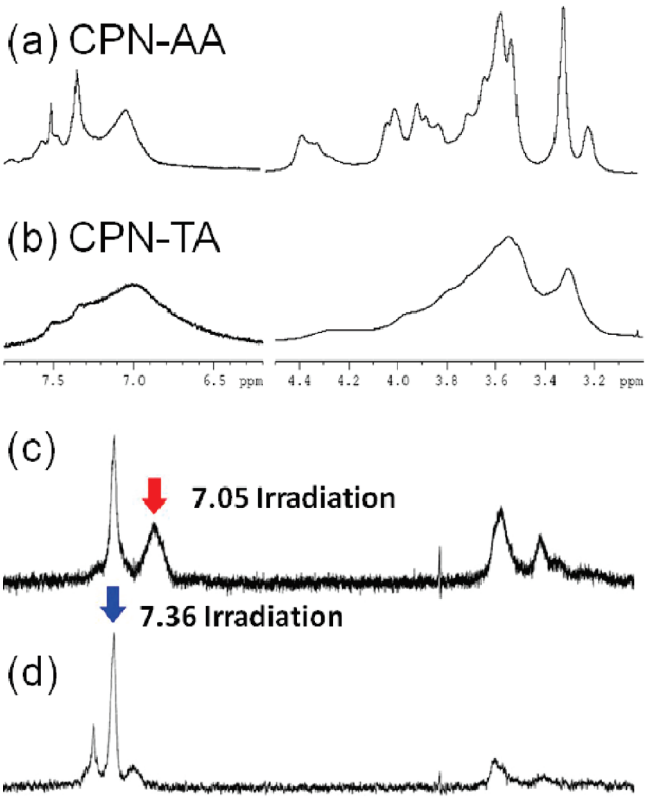

Figure 3. NMR spectra of CPN-AA (a), CPN-TA (b), and selective NOESY spectra of CPN-AA: 7.05 ppm (c) and 7.36 ppm (d) irradiation. NMR spectra indicate that the aggregation statuses are different between the organic acid treatments.

as shown in Figure 3, the degree of aggregation was significantly different between the acid treatments. The CPN-AAs exhibit relatively resolved proton peaks (Figure 3a), while the proton peaks in the CPN-TAs are heavily aggregated (Figure 3b). Three distinctively separated aromatic protons peaks were observed from the CPN-AAs, while a very broad aromatic proton peak with two shoulders was seen from the CPN-TAs. Generally, protons of CPs are broadened and upfield shifted due to the restricted rotational and translational motions in the aggregation.[39] From the broad aromatic proton and heavily aggregated side chain proton peaks, the backbones and side chains of the CPN-TAs are more tightly aggregated than those of the CPN-AAs. Meanwhile, well-solvated CPs generally exhibit downfield chemical shifts (i.e., deshielded) and relatively sharp aromatic proton peaks.[40] The CPN-AAs exhibit two relatively sharp aromatic peaks centered at 7.36 and 7.56 ppm along with a broad aggregation peak at 7.05 ppm. Selective nuclear Overhauser enhancement spectroscopy (NOESY) experiments clearly indicate that the aromatic protons interact strongly with each other through space. As shown in Figure 3c, the deshielded peak at 7.36 ppm appeared when the 7.05 ppm peak was irradiated, implying that the aromatic protons within the same aggregate but different aggregation structures are interacting through space. Interestingly, the sharp 7.56 ppm peak appeared along with the 7.05 ppm peak when the 7.36 ppm peak was irradiated (Figure 3d). No direct interaction between the peaks at 7.56 and 7.05 ppm through space was observed. The three aromatic environments can be interpreted as a core−shell-like structure with loose aggregation. The PPEs-NH_3^+ in the middle shell is relatively well solvated (deshielded) with direct communication with both the core (shielded) and shell (deshielded). Concentration dependent NMR experiments also support that the aromatic peaks originated from the same aggregates, not from a mixture of CPNs with isolated PPE-NH_2 chains (Supporting Information). The integration ratio of the 7.36 ppm peak to the 7.05 ppm peak increases as the CPNs concentration decreases. If the deshielded peaks originated from the isolated PPE-NH_3^+ (i.e., they are not parts of the CPN-AAs), the ratios would remain constant regardless of the dilutions. At lower concentration, the interpolyelectrolytes' attraction will be reduced while the hydrated chain proportion increases. Relatively, the concentration effect on the aromatic proton peaks of the CPN-TAs is minimal, indicating that the interpolymer hydrophobic interaction is somewhat strong. The difference in hydrophobic interaction between the CPN-AA and CPN-TA was examined by monitoring the change in the proportion of the aromatic protons while increasing organic solvent concentration (i.e., titration with CH_3OD). Because an organic solvent will reduce the hydrophobic interaction among aggregated chains, the proportion of the deshielded peaks will be increased from the loose aggregates. Indeed, the ratio changes were observed from both CPNs (Supporting Information). A dramatic increase in the ratio was observed in the CPN-AA. Almost all the shielded peaks disappeared at 50% CH_3OD concentration. However, the CPN-TAs still exhibit a significant intensity of the broad peak at the same MeOD concentration, implying the aggregation nature of the CPN-TAs is somewhat tight and strong. The NMR data support well the mechanistic interpretation that the low molecular weight proportions in the CPN-AAs were formed via a micelle-like mechanism since the aggregation characteristics are concentration, temperature, and counteranion. The dense aggregation was further tested by a fluorescence quenching experiment. Densely packed CPN-TAs exhibit a higher Stern−Volmer constant ($K_{SV} = 8 \times 10^4$) than that of the CPN-AA ($K_{SV} = 4 \times 10^4$) (Supporting Information).

On the basis of these results, we postulate two possible aggregation structures from the acid treatments, as shown in Figure 1. The loose aggregates of rigid rods of the PPE-NH_2 were built by reflecting blue-shifted absorption, relatively narrow emission, large hydrodynamic radius, and large concentration and solvent dependent proton NMR peaks. The dense or tight aggregation in the CPN-TAs was expressed by a high proportion of $\pi-\pi$ stacked PPE chains and packed assembly.

In conclusion, we have demonstrated that aggregation structure in CPNs can be modulated by different organic acids treatments using various spectroscopic techniques. Acetic acid offers loose aggregation in the CPNs, while tartaric acid produces dense and tight aggregation. The different aggregation states of CPNs showed the different physical and photophysical properties, leading to different applications. The loosely aggregated CPN-AAs are useful for delivery of drugs or biologically active molecules because they offer large surface area for encapsulation within the polymer chains. Recently, the CPN-AAs were used to complex negatively charged small interfering RNA (siRNA), and the complexes were successfully delivered siRNA to live cells to down regulate a target gene.[41] The densely aggregated CPN-TAs can be useful for sensing or labeling applications because the ordered $\pi-\pi$ stacking will offer more efficient energy transfer compared to the randomly organized aggregation. Fluorescent labeling of target cells or tissues with fewer environmental variations in the fluorescent signals can be expected by using

the tight aggregation. In this case, aggregation enhanced fluorescence should be considered to achieve high QYs.[42,43]

■ ASSOCIATED CONTENT

Supporting Information. Detailed experimental procedures, DLS, NMR, and Stern−Volmer plot. This material is available free of charge via the Internet at http://pubs.acs.org.

■ AUTHOR INFORMATION

Corresponding Author
*E-mail: jmoon@fiu.edu.

■ ACKNOWLEDGMENT

J.H.M. acknowledges FIU faculty startup fund. E.M. is supported by NIH/NIGMS R25 (EM061347).

■ REFERENCES

(1) Kim, I. B.; Shin, H.; Garcia, A. J.; Bunz, U. H. F. *Bioconjugate Chem.* **2007**, *18*, 815–820.
(2) Moon, J. H.; McDaniel, W.; MacLean, P.; Hancock, L. E. *Angew. Chem., Int. Ed.* **2007**, *46*, 8223–8225.
(3) Wu, C. F.; Szymanski, C.; Cain, Z.; McNeill, J. *J. Am. Chem. Soc.* **2007**, *129*, 12904–12905.
(4) Rahim, N. A. A.; McDaniel, W.; Bardon, K.; Srinivasan, S.; Vickerman, V.; So, P. T. C.; Moon, J. H. *Adv. Mater.* **2009**, *21*, 3492–3496.
(5) Pecher, J.; Huber, J.; Winterhalder, M.; Zumbusch, A.; Mecking, S. *Biomacromolecules* **2010**, *11*, 2776–2780.
(6) Pu, K. Y.; Li, K.; Liu, B. *Chem. Mater.* **2010**, *22*, 6736–6741.
(7) Howes, P.; Green, M.; Levitt, J.; Suhling, K.; Hughes, M. *J. Am. Chem. Soc.* **2010**, *132*, 3989–3996.
(8) Gaylord, B. S.; Heeger, A. J.; Bazan, G. C. *Proc. Natl. Acad. Sci. U.S.A.* **2002**, *99*, 10954–10957.
(9) Dore, K.; Dubus, S.; Ho, H. A.; Levesque, I.; Brunette, M.; Corbeil, G.; Boissinot, M.; Boivin, G.; Bergeron, M. G.; Boudreau, D.; Leclerc, M. *J. Am. Chem. Soc.* **2004**, *126*, 4240–4244.
(10) Miranda, O. R.; You, C. C.; Phillips, R.; Kim, I. B.; Ghosh, P. S.; Bunz, U. H. F.; Rotello, V. M. *J. Am. Chem. Soc.* **2007**, *129*, 9856–9857.
(11) Wosnick, J. H.; Mello, C. M.; Swager, T. M. *J. Am. Chem. Soc.* **2005**, *127*, 3400–3405.
(12) Rininsland, F.; Xia, W. S.; Wittenburg, S.; Shi, X. B.; Stankewicz, C.; Achyuthan, K.; McBranch, D.; Whitten, D. *Proc. Natl. Acad. Sci. U.S.A.* **2004**, *101*, 15295–15300.
(13) Bajaj, A.; Miranda, O. R.; Kim, I. B.; Phillips, R. L.; Jerry, D. J.; Bunz, U. H. F.; Rotello, V. M. *Proc. Natl. Acad. Sci. U.S.A.* **2009**, *106*, 10912–10916.
(14) Disney, M. D.; Zheng, J.; Swager, T. M.; Seeberger, P. H. *J. Am. Chem. Soc.* **2004**, *126*, 13343–13346.
(15) Lu, L. D.; Rininsland, F. H.; Wittenburg, S. K.; Achyuthan, K. E.; McBranch, D. W.; Whitten, D. G. *Langmuir* **2005**, *21*, 10154–10159.
(16) Thomas, S. W.; Joly, G. D.; Swager, T. M. *Chem. Rev.* **2007**, *107*, 1339–1386.
(17) Bunz, U. H. F. *Chem. Rev.* **2000**, *100*, 1605–1644.
(18) Arnrutha, S. R.; Jayakannan, M. *J. Phys. Chem. B* **2008**, *112*, 1119–1129.
(19) Breitenkamp, R. B.; Tew, G. N. *Macromolecules* **2004**, *37*, 1163–1165.
(20) Burrows, H. D.; Fonseca, S. M.; Silva, C. L.; Pais, A.; Tapia, M. J.; Pradhan, S.; Scherf, U. *Phys. Chem. Chem. Phys.* **2008**, *10*, 4420–4428.
(21) Garcia, A.; Nguyen, T. Q. *J. Phys. Chem. C* **2008**, *112*, 7054–7061.
(22) Kaur, P.; Yue, H. J.; Wu, M. Y.; Liu, M.; Treece, J.; Waldeck, D. H.; Xue, C. H.; Liu, H. Y. *J. Phys. Chem. B* **2007**, *111*, 8589–8596.
(23) Nguyen, T. Q.; Doan, V.; Schwartz, B. J. *J. Chem. Phys.* **1999**, *110*, 4068–4078.
(24) Lee, K.; Cho, J. C.; DeHeck, J.; Kim, J. *Chem. Commun.* **2006**, 1983–1985.
(25) Kitchens, K. M.; Foraker, A. B.; Kolhatkar, R. B.; Swaan, P. W.; Ghandehari, H. *Pharm. Res.* **2007**, *24*, 2138–2145.
(26) vandeWitte, P.; Dijkstra, P. J.; vandenBerg, J. W. A.; Feijen, J. *J. Membr. Sci.* **1996**, *117*, 1–31.
(27) Gelbart, W. M., Ben-Shaul, A., Roux, D., Eds.; *Micelles, Membranes, Microemulsions, and Monolayers*; Srpinger: New York, 1994.
(28) Yang, R. Q.; Garcia, A.; Korystov, D.; Mikhailovsky, A.; Bazan, G. C.; Nguyen, T. Q. *J. Am. Chem. Soc.* **2006**, *128*, 16532–16539.
(29) Tan, C.; Atas, E.; MÃ1/4ller, J. r. G.; Pinto, M. R.; Kleiman, V. D.; Schanze, K. S. *J. Am. Chem. Soc.* **2004**, *126*, 13685–13694.
(30) Liu, B.; Bazan, G. C. *J. Am. Chem. Soc.* **2004**, *126*, 1942–1943.
(31) Satrijo, A.; Swager, T. M. *J. Am. Chem. Soc.* **2007**, *129*, 16020–16028.
(32) The shapes of emission spectra are quite different among different batches, while the same aggregation patterns from the treatments were observed. The absorption spectra of the CPNs exhibit no significant batch-to-batch variations. Difference in the emission spectra can be attributed to the molecular weight variations among the different batches, so that aggregation behaviors are slightly different. This observation indicates indirectly that the CPN formation is driven by micelle formation, which the processes are governed by molecular weight.
(33) Kim, J.; Swager, T. M. *Nature* **2001**, *411*, 1030–1034.
(34) Barbara, P. F.; Gesquiere, A. J.; Park, S. J.; Lee, Y. J. *Acc. Chem. Res.* **2005**, *38*, 602–610.
(35) VanVeller, B.; Miki, K.; Swager, T. M. *Org. Lett.* **2010**, *12*, 1292–1295.
(36) Garcia, F.; Fernandez, G.; Sanchez, L. *Chem.—Eur. J.* **2009**, *15*, 6740–6747.
(37) Justino, L. L. G.; Ramos, M. L.; Abreu, P. E.; Carvalho, R. A.; Sobral, A.; Scherf, U.; Burrows, H. D. *J. Phys. Chem. B* **2009**, *113*, 11808–11821.
(38) Jones, T. V.; Slutsky, M. M.; Laos, R.; de Greef, T. F. A.; Tew, G. N. *J. Am. Chem. Soc.* **2005**, *127*, 17235–17240.
(39) Collison, C. J.; Rothberg, L. J.; Treemaneekarn, V.; Li, Y. *Macromolecules* **2001**, *34*, 2346–2352.
(40) Lahiri, S.; Thompson, J. L.; Moore, J. S. *J. Am. Chem. Soc.* **2000**, *122*, 11315–11319.
(41) Silva, A. T.; Alien, N.; Ye, C. M.; Verchot, J.; Moon, J. H. *BMC Plant Biol.* **2010**, *10*, 291.
(42) Kokado, K.; Chujo, Y. *Macromolecules* **2009**, *42*, 1418–1420.
(43) Satrijo, A.; Kooi, S. E.; Swager, T. M. *Macromolecules* **2007**, *40*, 8833–8841.